Speech recognition through physical reservoir computing with neuromorphic nanowire networks

Speech recognition through physical reservoir computing with neuromorphic nanowire networks

1st Gianluca Milano
Advanced Materials Metrology and Life Sciences Division
INRiM (Istituto Nazionale di Ricerca Metrologica)
Strada delle Cacce 91, 10135 Torino,
Italy g.milano@inrim.it

4th Carlo Ricciardi
Department of Applied Science and Technology
Politecnico di Torino
C.so Duca degli Abruzzi 24, 10129 Torino, Italy carlo.ricciardi@polito.it

2nd Matteo Agliuzza
Department of Applied Science and Technology
Politecnico di Torino
C.so Duca degli Abruzzi 24, 10129 Torino, Italy matteo.agliuzza@polito.it

3rd Natascia De Leo
Advanced Materials Metrology and Life Sciences Division
INRiM (Istituto Nazionale di Ricerca Metrologica)
Strada delle Cacce 91, 10135 Torino,
Italy n.deleo@inrim.it

***Abstract* — The hardware implementation of the reservoir computing paradigm represents a key aspect for taking into advantage of neuromorphic data processing. In this context, self-organised nanonetworks represent a versatile and scalable computational substrate for multiple tasks by exploiting the emerging collective behaviour of the system arising from complexity. The emerging behaviour allows spatio-temporal processing of multiple input signals and relies on the nonlinear interaction in between a multitude of nanoscale memristive elements. By means of a physics-based grid-graph modeling, we report on the implementation of reservoir computing for a speech recognition task in a memristive nanonetwork based on nanowires (NWs) acting as a physical reservoir. Besides analysing the pre-processing step for the transduction of the audio samples in electrical stimuli to be applied to the physical reservoir, we analyse the effect of the network size and the adoption of virtual nodes on computing performances. Results show that memristive nanonetworks allow *in materia* implementation of reservoir computing for the realisation of brain-inspired neuromorphic systems with reduced training cost.**

Keywords — physical reservoir, reservoir computing, speech recognition, memristive network, nanowire networks

I. INTRODUCTION

Neuromorphic computing aims to overcome main limitations of the conventional von Neumann computing architecture, where the continuous and intensive interchange of data in between memory and processing units that are implemented in separate blocks is responsible for a large part of the power consumption of the system. In this context, the development of neuromorphic computing and engineering rely on the development of new hardware technologies and architectures mimicking functionalities and effectiveness of biological neuronal circuits [1], [2].

Among emerging devices and technologies, memristive devices represent one of the most promising candidates for the development of biologically-plausible architectures able to storage and process information in the same physical location [3]. Memristive devices are two-terminal devices where the internal state of resistance depends on the history of applied voltage and current [4], [5]. For this reason, these devices that couples ionics with electronics, have been exploited as building blocks for emulating neuronal and synaptic functionalities [6]–[8]. In this framework, large arrays of memristive devices, fabricated with a top-down approach through lithographic techniques, have been exploited for the realisation of artificial neural networks and brain-inspired systems [9], [10].

Inspired by self-organisation processing regulating both the topology and functions of biological neuronal circuits, self-assembled complex nanonetworks of memristive elements have been recently demonstrated for physical implementation of neuromorphic-type of information processing [11]–[20]. Differently from top-down architectures, functionalities of self-organizing networks emerge from the collective behaviour and interactions in between a huge number of nano elements without the need of fine tuning of each part of the system [21]. Among nanonetworks, randomly displaced nanowires (NWs) forming an highly interconnected network have been demonstrated to exhibit a wide range of collective neural-like dynamics including short-term and long-term plasticity, heterosynaptic plasticity, avalanche effects, criticality and edge-of-chaos [11]–[14]. By exploiting these dynamics, memristive NW networks have been proposed as versatile substrates for

in materia implementation of reservoir computing (RC) [22]– [27]. The major advantage of RC, derived from recurrent neural network models and allowing temporal and sequential data processing, relies on the fast learning and low training cost. This is because an RC system is composed of a reservoir that maps inputs in a feature space that is then analysed by a readout that is the only part that needs to be trained [28], [29].

In this work, we report on physics-based simulations of the implementation of RC for speech recognition in neuromorphic NW networks. Besides reporting on the implementation of RC by exploiting the emergent dynamics of the NW network, pre-processing for the transduction of the audio signal into electrical stimuli through the Lyon's auditory model is analysed. Also, the effect of the network size and the role of virtual nodes on computing performances are discussed. The results show that the emergent dynamics of NW networks can be exploited for the realisation of neuromorphic systems able to process multiple spatio-temporal input signals.

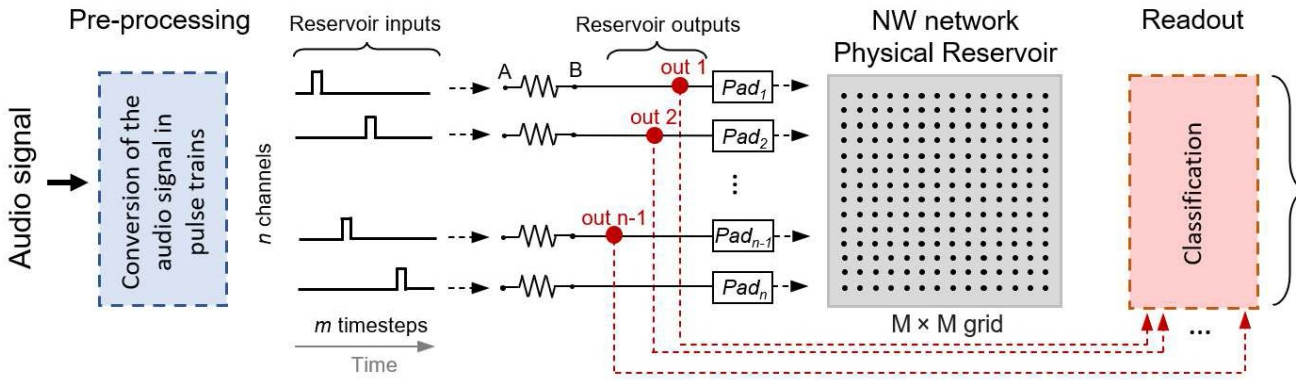

Fig. 1. Conceptual schematic representation of physical implementation of reservoir computing (RC) for speech recognition with neuromorphic NW networks. The computing implementation involves three steps: *i)* pre-processing, *ii)* non-linear transformation by the NW network reservoir and *iii)* classification of reservoir outputs by the readout. Pre-processing step involves the conversion of the audio signal in pulse trains that are then applied to terminals *A* of *n* channels, where each channel is connected to a pad contacting the NW network physical reservoir. Voltages of *n-1* channels measured at terminals *B* of the resistance *R* represent the reservoir outputs that are then passed to the readout for classification.

II. Results and Discussion

A conceptual schematisation of the physical implementation of reservoir computing in NW networks is reported in Fig. 1. The implementation involves mainly three steps: *i)* pre-processing of the input signal, *ii)* non-linear transformation of the input through the physical NW network reservoir, and *iii)* classification of the reservoir outputs performed by the readout. NW networks can be realised by simply drop-casting Ag NWs surrounded by an insulating shell of polyvinylpyrrolidone (PVP) in solution on an insulating substrate. By means of this technique, a highly interconnected network of randomly dispersed NWs over a large scale (~ cm^2) can be obtained [11], [30], [31]. The typical topology of an Ag NW network realised on a SiO_2 insulating substrate is reported in the Scanning Electron Microscopy (SEM) image of Fig. 2.

A. Pre-processing of the audio signal

A pre-processing step is required to convert the audio signal (Fig. 3a) in electrical stimuli to be applied to the physical reservoir. This process emulates the transduction mechanism of the human ears that transform sound waves in nerve pulses then transferred to the brain wherein they are recognised and processed. By emulating the most important cochlea's functions, the Lyon's Auditory model [32] has been exploited for pre-processing of the audio signal. This technique allows the extraction of features of input time- varying signal in the frequency rather than in the amplitude domain. In the first stage, the frequency components of the acoustic waves are separated. Then, a detection stage simulates the hair cell detection of the basilar membrane in the cochlea and a final compression stage is exploited to regulate the output's dynamic range. The output of the Lyon's model is represented by the so-called cochleagram (Fig. 3b) that, similarly to a spectrogram, represents the intensity of the hair cells activity over time. Then, the cochleagram is interpolated (one-dimensional piecewise linear interpolation), discretised and binarised. After normalisation of the cochleagram in the range (0,1), binarisation was performed by choosing a threshold value of 0.6. The resulting spatio-temporal pattern representing the cochleagram (Fig. 3c) is composed of n channels and m timestamps with white (0) or black (1) pixels.
This n × m input represents a spatio-temporal reservoir input composed of n spatial inputs (channels) each containing m timeframes. Each spatial input corresponds to a train of pulses applied to a different pad of the network, where each timeframe with a width of 11 ms is composed of a 10 ms pulse of 5 V if corresponding to a black pixel or to 0 V if corresponding to a white pixel followed by 1 ms biased at 0 V. Note that the binarisation and the following transformation of the cochleagram into streams of pulses can be interpreted as the production of electrical stimuli in form of pulses from the hair cells of the ears when the received signal from the cochlea is strong enough (i.e. when it exceeds a threshold value). This train of pulses is then applied to different locations of the NW network reservoir through electrodes acting as neuron terminals disposed on M × M grid-like fashion. In this context, it is worth noticing that the acoustic transformation during the pre-processing plays a critical role in feature extraction and, thus, represents an important aspect to be considered during the evaluating performances of the RC system [33].

B. Emerging behaviour of the physical reservoir

The neuromorphic NW network is exploited as a physical reservoir for a non-linear transformation of the input signal by exploiting its emerging memristive behaviour. This emerging behaviour is related to the mutual interaction of memristive NW junctions composing the network.

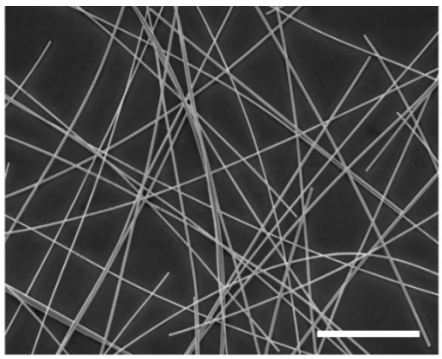

Fig. 2. Scanning Electron Microscopy (SEM) image of an Ag NW network realised by drop-casting on a SiO_2 insulating substrate (scale bar, 5 μm).

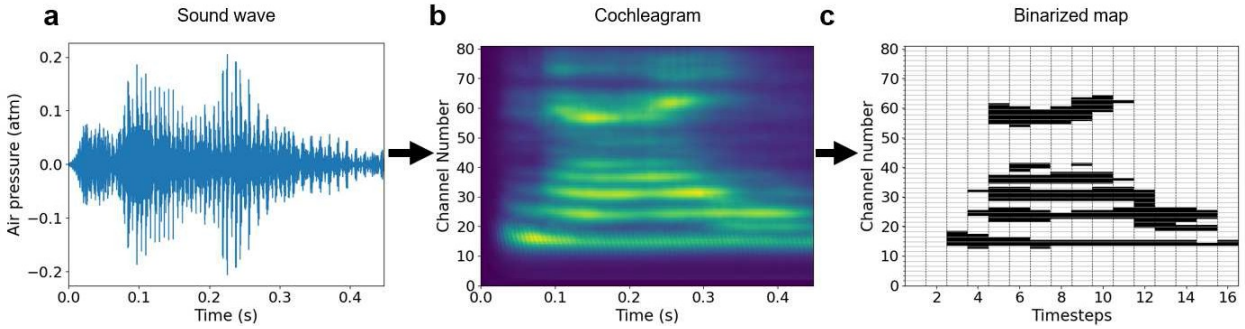

Fig. 3. Pre-processing of the input signal. (a) Example of a sound wave corresponding to a spoken digit nine and (b) corresponding cochleagram where each channel on the y-axis represents a frequency window in the range from 0 to 4 kHz (higher index channels correspond to higher frequencies). (c) Corresponding spatio-temporal pattern composed of n channels and k timesteps representing the cochleagram after interpolation, discretisation and binarisation.

The memristive behavior in NW junctions rely on the so-called resistive switching mechanism that is responsible for the formation of a conductive filament connecting the two intersecting NW cores under the action of the applied electric field, lowering the overall junction resistance. This switching mechanism is volatile, meaning that the metallic filament spontaneously dissolves after the end stimulation. A detailed analysis of the switching mechanism in single network elements can be found in a previous work [11]. The formation and dissolution of filaments at NW junctions are responsible for a network-wide memristive behaviour that allows spatio - temporal processing of the input signal by exploiting the emergent nonlinear dynamics and fading memory properties of the neuromorphic reservoir network. The emergent spatio- temporal dynamics can be emulated through grid-graph modelling [22], [34]. In this context, the NW network topology is represented as a regular grid-graph. This assumption holds in case of high-density NW networks that can be approximated as a continuous conductive medium. The memristive short-term dynamics of graph edges are modelled with one equation for the memory state and one equation to describe the electron transport, according to a previous work [35].
The dynamics of the memory state g (i.e. the normalized edge conductance) are described through a physics-based potentiation-depression rate balance equation:

$$\frac{dg}{dt} = k_p(1-g) + k_d g$$

where k_p and k_d are the potentiation and depression coefficients (that are defined as a function of the voltage difference in between nodes connected by the edge [35]). This equation can be recursively solved as detailed in ref. [35]. Instead, the electron transport is described according to the first Ohm's law through the equation:

$$I(t) = \left[G_{min}\big(1-g(t)\big) + G_{max}\big(g(t)\big)\right]V(t)$$

where G_{min} and G_{max} are the minimum and maximum of conductance, respectively. Model parameters were retrieved from interpolation of experimental data [22]. For each simulation timestep, the voltage at each node and current flowing in each edge was calculated through the modified voltage node analysis and the edge conductance (memory state) is updated. During stimulation, reservoir inputs in the form of pulse trains are applied to terminals *A* of the n reservoir input channels (refer to Fig. 1). Each input channel corresponds to a terminal neuron located in a different area of the NW network, with terminals disposed on a M × M grid-like fashion. The reservoir output is represented by the set of the output voltages measured at terminals *B* of the resistance *R* while a small bias voltage is applied to a selected arbitrary channel (read electrode) while terminal *A* of all other channels are grounded.
Note that this configuration described in detail in ref. [22] allows to exploit the same electrodes both as inputs and outputs of the physical reservoirs, reducing the overall number of terminal electrodes.

Grid-graph modelling allows direct visualisation of emerging nonlinear dynamics exploited for temporal processing of multiple spatial inputs, as reported in Fig. 4a. Here, the evolution over timesteps of the NW network under stimulation with the spatio-temporal pattern shown in Fig. 3c is reported. As can be observed, the multiterminal stimulation is responsible for a spatio-temporal evolution of the NW network conductivity map over timesteps that depends on the spatial location as well as on the specific temporal sequence of stimulating voltage pulses. It is worth noticing that the competition in between potentiation of stimulated areas and subsequent spontaneous relaxation to the ground state endow the NW network with the accumulation capability, that is the capacity of progressively increasing the conductance of network areas that are stimulated with temporally correlated voltage pulses. In this framework, the dynamics of the reservoir outputs reflects the peculiar evolution of the NW network conductivity map. The temporal evolution of reservoir outputs resulting from the dynamics visualised in Fig. 4a is reported in Fig. 4b, where the temporal evolution of some selected outputs is shown. The reservoir outputs are the result of a non-linear transformation of the input signals resulting from memristive dynamics with fading memory properties of the system.

C. Readout classification

The final reservoir states (i.e. the reservoir state after the end of stimulation) represented by the set of n-1 independent output voltages (output vector) can be then passed to the readout for classification. Note that the readout is the only part of the system that needs to be trained. Before being fed to the readout, reservoir output voltages were standardised by removing the mean value and scaling to the unit variance.

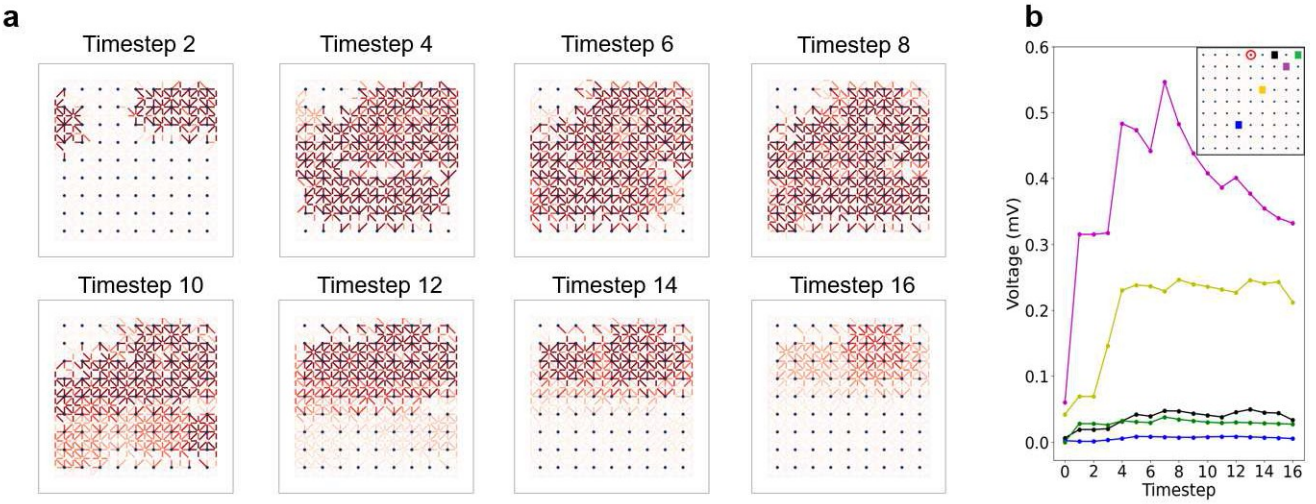

Fig. 4 Evolution of the NW network physical reservoir state. (a) Direct visualisation of the evolution over timesteps of the NW network reservoir state represented during stimulation with the spatiotemporal pattern representing the cochleagram corresponding to a digit nine reported in Fig. 3c, and (b) corresponding evolution of selected output timetraces (selected channels highlighted in the inset, where the read electrode is circled in red.

In addition, in order to overcome the loss of information from the far-history of the input, the virtual node processing concept was exploited [36]. This means that not only the reservoir state after the end of stimulation but also intermediate reservoir states are passed to the readout. Given *i* the number of considered virtual nodes, the size of the output vector will be i(n-1). In other words, adding a virtual node means to pass to the readout an additional set of n -1 independent output voltages measured at an intermediate timestep, thus virtually increasing the reservoir size. Given an input with *m* timesteps, considering *i* virtual nodes means to pass to the readout the set of output voltages acquired every *m/i* timesteps. It is important to highlight that the case of $i = 1$ corresponds to the case where only the set of output voltages at the end of stimulation are passed to the readout (i.e. only the final reservoir state is considered for classification). Note that an increase of virtual nodes results also in a larger number of parameters to be trained at the readout. The readout function is implemented through a logistic regression algorithm, where the weighted sum of the reservoir outputs is transformed by a sigmoid function in a categorical value in the range (0,1), which brings information about the probability of the input of belonging to a particular class.

D. Speech recognition with a physical reservoir

The computing capabilities of the reservoir computing system based on the neuromorphic NW network physical reservoir have been evaluated on the speech recognition task. For this purpose, pre-processed audio samples are mapped into reservoir states (i.e. output voltages) and then classified by the readout following as previously described. Computing performances have been evaluated by considering the free- spoken digit dataset (Tensorflow) [37]. This dataset consists of audio samples of digits from 0 to 9 pronounced by 6 different speakers. Each speaker is recorded 50 different times for each digit, resulting in a total of 3000 audio samples. The readout was trained on 2700 audio files and tested with the remaining 300 audio samples (30 audio samples for each digit) by exploiting the *k*-fold cross validation technique ($k = 10$ was considered).

Fig. 5a reports the accuracy of the system achieved by considering different numbers of virtual nodes. Results have been obtained by considering n = 81 channels (i.e. 81 terminal neurons connecting the NW network) and m = 16 timesteps during pre-processing. Here, the accuracy of the reservoir-based system is compared to the accuracy of the system without

reservoir (i.e. the pre-processed data fed directly to the readout). We point out that this comparison is crucial to understand the effective advantages of the physical reservoir system.

Firstly, results evidenced that the reservoir-based system achieve a higher accuracy. This is because the non-linear transformation of the input performed by the reservoir with short-term memory extracts spatio-temporal correlations of the input signals with consequence increase of the system accuracy. Secondly, it can be observed that the accuracy progressively increases by increasing the number of virtual nodes. Indeed, an increasing number of virtual nodes can balance the loss of information from initial stimulation timesteps due to the short-term memory of the physical reservoir. Notably, it is important to remark that an higher gain of accuracy respect to the system without the reservoir can be observed for a reduced number of virtual nodes. This means that the gain of accuracy with the reservoir is higher when a lower amount of parameters have to be trained in the readout.

The accuracy of the system obtained by progressively increasing the reservoir size in terms of the number *n* of electrodes is reported in Fig. 5b, where results have been obtained by fixing the number of timesteps to m = 16 and the virtual nodes to i = 2. Note that an increasing the number of electrodes strongly impacts also the pre-processing step since this means to increase the number of channels extracted from the cochleagram accordingly. As can be observed, the accuracy of the system increases by increasing the number of electrodes. This is because an increased number of channels corresponds to a binarised spatio-temporal pattern obtained from the corresponding cochleagram with enhanced resolution in frequencies, thus resulting in a reservoir input pattern that endows an increased amount of information on the original audio signal.

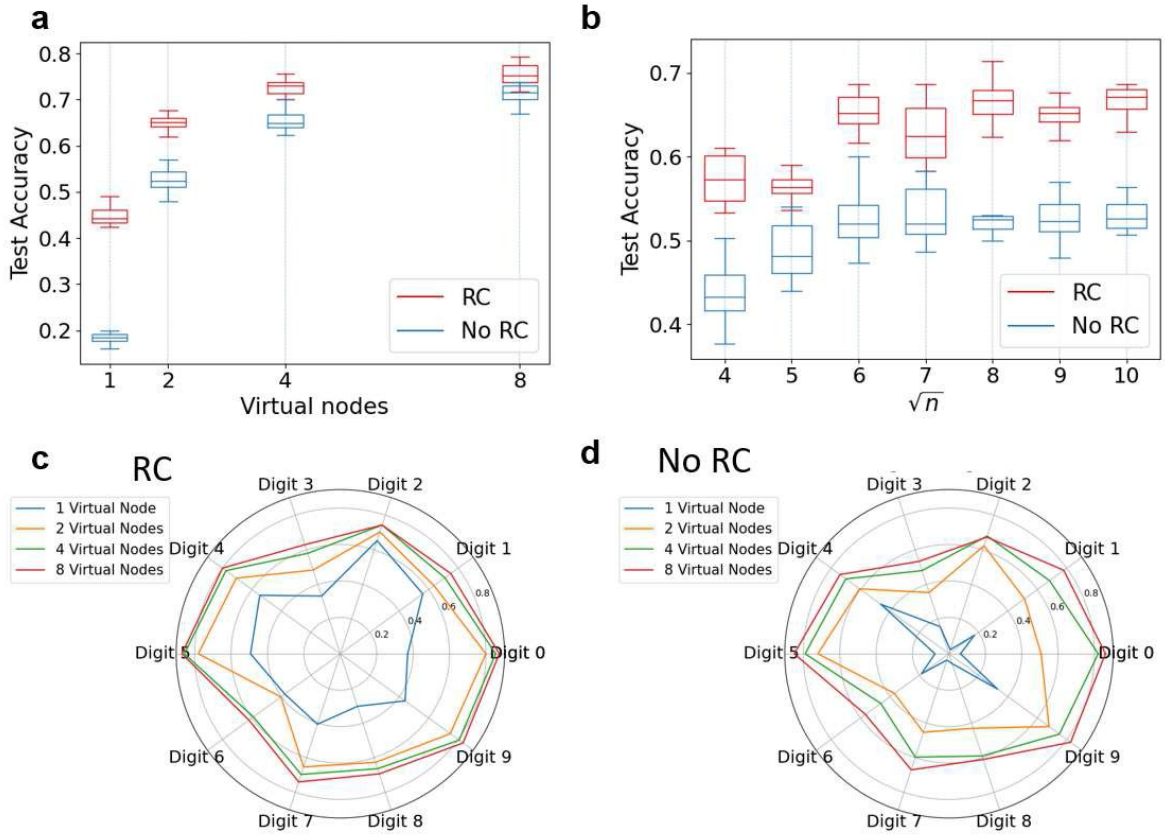

Fig. 5 Speech recognition with neuromorphic NW networks as physical reservoir. (a) Accuracy of the system as a function of the number of considered virtual nodes. (b) Accuracy of the system as a function of the number of input electrodes *n* by considering 2 virtual nodes. Results in panels (a) and (b) are compared with results obtained without the physical reservoir, and box plots were retrieved from results obtained with the *k*-fold cross validation technique with $k = 10$. (c,d) Charts representing the accuracy for digit recognition of the system by taking into account different numbers of virtual nodes with and without physical reservoir, respectively.

However, it is worth noticing that for $\sqrt{n} > 7$ the accuracy of the system tends to saturate. This is related to the fact that no further relevant features of the cochleogram are extracted by further increasing its frequency resolution (i.e. by increasing the number of channels) during pre-processing. Importantly, in all cases the reservoir-based system accuracy outperforms the system without a reservoir.

For the sake of completeness, charts reported in Fig. 5c shows the ability of the RC system to correctly estimate the target digit. It can be clearly visualized that the ability to correctly classify the target digit increases by progressively increasing the number of virtual nodes. As a comparison, Fig. 5d shows the same chart of the computing system without reservoir that, by comparing results obtained with the same number of virtual nodes, shows lower computing performances.

In perspective, the accuracy of the system can be further improved by properly adjusting the nonlinear response and dynamics of the NW networks through *i)* adjustment of the NW network density and *ii)* an engineering of the core-shell NW structure. Also, it is worth noticing that this physical implementation of RC can be extended not only to other temporal tasks but also for computing tasks where the temporal dynamics of input signals are coupled with spatial information.

III. Conclusions

In conclusion, we have shown with physics-based simulations that the neuromorphic NW network can be exploited as a physical substrate for a speech recognition computing task through the implementation of RC. In particular, the NW network acts as a physical reservoir thanks to its nonlinear dynamics, fading memory properties and its capability of processing multiple spatio-temporal inputs. Pre- processing and transduction of the input audio signal was analysed and discussed together with an analysis of the effect of network size and virtual nodes on computing performances. Results suggest that the NW network can be exploited for the hardware realisation of neuromorphic systems able to solve spatio-temporal computing tasks.

Acknowledgment

This work was supported by the European project MEMQuD, code 20FUN06. This project (EMPIR 20FUN06 MEMQuD) has received funding from the EMPIR programme co-financed by the Participating States and from the European Union's Horizon 2020 research and innovation programme.

References

[1] D. V. Christensen *et al.*, "2022 roadmap on neuromorphic computing and engineering," *Neuromorphic Comput. Eng.*, vol. 2, no. 1, pp. 0–31, Jan. 2022.

[2] K. Berggren *et al.*, "Roadmap on emerging hardware and technology for machine learning," *Nanotechnology*, vol. 32, no. 1, p. 012002, Jan. 2021.

[3] R. Waser, Ed., *Nanoelectronics and Information Technology: Materials, Processes, Devices*, 3rd ed. John Wiley & Sons, 2012.

[4] Z. Wang *et al.*, "Resistive switching materials for information processing," *Nat. Rev. Mater.*, vol. 5, no. 3, pp. 173–195, Mar. 2020.

[5] D. B. Strukov, G. S. Snider, D. R. Stewart, and R. S. Williams, "The missing memristor found," *Nature*, vol. 453, no. 7191, pp. 80–83, May 2008.

[6] J. Tang *et al.*, "Bridging Biological and Artificial Neural Networks with Emerging Neuromorphic Devices: Fundamentals, Progress, and Challenges," *Adv. Mater.*, vol. 31, no. 49, p. 1902761, Dec. 2019.

[7] G. Milano *et al.*, "Self-limited single nanowire systems combining all-in-one memristive and neuromorphic functionalities," *Nat. Commun.*, vol. 9, no. 1, p. 5151, Dec. 2018.

[8] S. H. Jo, T. Chang, I. Ebong, B. B. Bhadviya, P. Mazumder, and W. Lu, "Nanoscale Memristor Device as Synapse in Neuromorphic Systems," *Nano Lett.*, vol. 10, no. 4, pp. 1297– 1301, Apr. 2010.

[9] Q. Xia and J. J. Yang, "Memristive crossbar arrays for brain- inspired computing," *Nat. Mater.*, vol. 18, no. 4, pp. 309–323, Apr. 2019.

[10] P. Lin *et al.*, "Three-dimensional memristor circuits as complex neural networks," *Nat. Electron.*, vol. 3, no. 4, pp. 225–232, Apr. 2020.

[11] G. Milano *et al.*, "Brain-Inspired Structural Plasticity through Reweighting and Rewiring in Multi-Terminal Self-Organizing Memristive Nanowire Networks," *Adv. Intell. Syst.*, p. 2000096, Jun. 2020.

[12] J. Hochstetter, R. Zhu, A. Loeffler, A. Diaz-Alvarez, T. Nakayama, and Z. Kuncic, "Avalanches and edge-of-chaos learning in neuromorphic nanowire networks," *Nat. Commun.*, vol. 12, no. 1, p. 4008, Dec. 2021.

[13] H. G. Manning *et al.*, "Emergence of winner-takes-all connectivity paths in random nanowire networks," *Nat. Commun.*, vol. 9, no. 1, p. 3219, Dec. 2018.

[14] A. Diaz-Alvarez *et al.*, "Emergent dynamics of neuromorphic nanowire networks," *Sci. Rep.*, vol. 9, no. 1, p. 14920, Dec. 2019.

[15] M. D. Pike *et al.*, "Atomic Scale Dynamics Drive Brain-like Avalanches in Percolating Nanostructured Networks," *Nano Lett.*, vol. 20, no. 5, pp. 3935–3942, May 2020.

[16] J. B. Mallinson, S. Shirai, S. K. Acharya, S. K. Bose, E. Galli, and S. A. Brown, "Avalanches and criticality in self-organized nanoscale networks," *Sci. Adv.*, vol. 5, no. 11, p. eaaw8438, Nov. 2019.

[17] R. Zhu *et al.*, "Information dynamics in neuromorphic nanowire networks," *Sci. Rep.*, vol. 11, no. 1, p. 13047, Dec. 2021.

[18] Z. Kuncic and T. Nakayama, "Neuromorphic nanowire networks: principles, progress and future prospects for neuro-inspired information processing," *Adv. Phys. X*, vol. 6, no. 1, Jan. 2021.

[19] G. Milano, S. Porro, I. Valov, and C. Ricciardi, "Recent Developments and Perspectives for Memristive Devices Based on Metal Oxide Nanowires," *Adv. Electron. Mater.*, vol. 5, no. 9, p. 1800909, Sep. 2019.

[20] G. Milano, E. Miranda, and C. Ricciardi, "Connectome of memristive nanowire networks through graph theory," *Neural Networks*, vol. 150, pp. 137–148, Jun. 2022.

[21] M. Aono and K. Ariga, "The Way to Nanoarchitectonics and the Way of Nanoarchitectonics," *Adv. Mater.*, vol. 28, no. 6, pp. 989– 992, Feb. 2016.

[22] G. Milano *et al.*, "In materia reservoir computing with a fully memristive architecture based on self-organizing nanowire networks," *Nat. Mater.*, vol. 21, no. 2, pp. 195–202, Feb. 2022.

[23] T. Kotooka *et al.*, "Ag 2 Se Nanowire Network as an Effective In-Materio Reservoir Computing Device," *Res. Sq.*, pp. 1–20, 2021.

[24] A. Loeffler *et al.*, "Modularity and multitasking in neuro- memristive reservoir networks," *Neuromorphic Comput. Eng.*, vol. 1, no. 1, p. 014003, Sep. 2021.

[25] R. Zhu *et al.*, "MNIST classification using Neuromorphic Nanowire Networks," in *International Conference on Neuromorphic Systems 2021*, 2021, pp. 1–4.

[26] A. Z. Stieg, A. V. Avizienis, H. O. Sillin, C. Martin-Olmos, M. Aono, and J. K. Gimzewski, "Emergent Criticality in Complex Turing B-Type Atomic Switch Networks," *Adv. Mater.*, vol. 24, no. 2, pp. 286–293, Jan. 2012.

[27] H. O. Sillin *et al.*, "A theoretical and experimental study of neuromorphic atomic switch networks for reservoir computing," *Nanotechnology*, vol. 24, no. 38, p. 384004, Sep. 2013.

[28] G. Tanaka *et al.*, "Recent advances in physical reservoir computing: A review," *Neural Networks*, vol. 115, pp. 100–123, Jul. 2019.

[29] K. Nakajima, "Physical reservoir computing—an introductory perspective," *Jpn. J. Appl. Phys.*, vol. 59, no. 6, p. 060501, Jun. 2020.

[30] G. Milano *et al.*, "Mapping Time-Dependent Conductivity of Metallic Nanowire Networks by Electrical Resistance Tomography toward Transparent Conductive Materials," *ACS Appl. Nano Mater.*, p. acsanm.0c02204, Oct. 2020.

[31] A. Cultrera, G. Milano, N. De Leo, C. Ricciardi, L. Boarino, and L. Callegaro, "Recommended implementation of electrical resistance tomography for conductivity mapping of metallic nanowire networks using voltage excitation," *Sci. Rep.*, vol. 11, no. 1, p. 13167, Dec. 2021.

[32] R. Lyon, "A computational model of filtering, detection, and compression in the cochlea," in *ICASSP '82. IEEE International Conference on Acoustics, Speech, and Signal Processing*, 1982, vol. 7, pp. 1282–1285.

[33] F. Abreu Araujo *et al.*, "Role of non-linear data processing on speech recognition task in the framework of reservoir computing," *Sci. Rep.*, vol. 10, no. 1, p. 328, Dec. 2020.

[34] K. Montano, G. Milano, and C. Ricciardi, "Grid-graph modeling of emergent neuromorphic dynamics and heterosynaptic plasticity in memristive nanonetworks," *Neuromorphic Comput. Eng.*, pp. 0–22, Jan. 2022.

[35] E. Miranda, G. Milano, and C. Ricciardi, "Modeling of Short- Term Synaptic Plasticity Effects in ZnO Nanowire-Based Memristors Using a Potentiation-Depression Rate Balance Equation," *IEEE Trans. Nanotechnol.*, vol. 19, pp. 609–612, 2020.

[36] L. Appeltant *et al.*, "Information processing using a single dynamical node as complex system," *Nat. Commun.*, vol. 2, no. 1, p. 468, Sep. 2011.

[37] Zohar Jackson; César Souza; Jason Flaks; Yuxin Pan; Hereman Nicolas; Adhish Thite, "Jakobovski/free-spoken-digit-dataset (FSDD) v1.0.08 (Accessed: April 2021), DOI: 10.5281/zenodo.1342401."